Compressive sensing based 3D imaging using a moving MIMO array

Liu, D.

TR2015-090 July 2015

Abstract

We consider a 3D configuration where a coherent cross-track MIMO radar with uniform spaced transmit-receive antennas is mounted on a moving platform. Given a restricted number of transmit channels and known motion errors, we propose to randomize the transmit channels and employ a compressive sensing (CS)-based imaging approach to reconstruct 3D images by exploiting sparsity of the scene to be reconstructed. Results on simulated data demonstrate that our proposed moving MIMO platform performs much better than that with the same number but fixed transmit channels in reconstructing 3D images, and close to that using full channel MIMO operation but with much fewer transmit channels.

2015 IEEE International Geoscience and Remote Sensing Symposium (IGARSS)

COMPRESSIVE SENSING BASED 3D IMAGING WITH A MOVING MIMO ARRAY

Dehong Liu

Mitsubishi Electric Research Labs
201 Broadway, Cambridge, MA 02139

ABSTRACT

We consider a 3D configuration where a coherent cross-track MIMO radar with uniform spaced transmit-receive antennas is mounted on a moving platform. Given a restricted number of transmit channels and known motion errors, we propose to randomize the transmit channels and employ a compressive sensing (CS)-based imaging approach to reconstruct 3D images by exploiting sparsity of the scene to be reconstructed. Results on simulated data demonstrate that our proposed moving MIMO platform performs much better than that with the same number but fixed transmit channels in reconstructing 3D images, and close to that using full channel MIMO operation but with much fewer transmit channels.

***Index Terms*—** MIMO imaging, 3D imaging, compressive sensing

1. INTRODUCTION

Conventional radar systems make use of wide-band signal and large aperture to generate high resolution radar images. With a linear array, one can generate 2D range-azimuth images without any elevation information. When a planar array is available for collecting radar echoes, 3D images in range-azimuth-elevation can be formed. The planar array can be a real planar array composed of antennas or a virtual array realized by either multiple passes of a single-channel platform [1] or a single pass of a multi-channel platform [2].

In recent years, multi-input multi-output (MIMO) system, as a moving multi-channel platform with 3D imaging capability, attracts great attention in radar imaging [3, 4]. Compared to single channel radar platforms, the degrees of freedom of MIMO are greatly increased by the multiple transmit-receive channels, resulting significantly improved elevation resolution. However, it is challenging to design independent transmit signals such that the radar echoes do not interfere each other during MIMO operation. Although the transmitted signals can be designed to be orthogonal to each other, the reflected echoes may inevitably interfere each other due to the lack of orthogonality [5, 6]. In addition, moving radar platforms typically exhibit motion errors due to speed variations in both direction and magnitude, forming nonuniform virtual arrays [2]. Consequently, ambiguity and defocus will be observed in radar images if the motion errors are not well compensated.

In this paper, we re-examine these fundamental challenges and propose a compressive sensing (CS) based moving MIMO array platform for 3D imaging. CS is a research topic that has gained great attention in the applied mathematics and signal processing communities in recent years [7]. It allows robust reconstruction of an underlying signal using a significantly smaller number of measurements compared to its Nyquist rate under the assumption that the signal to be reconstructed is sparse or compressible in some domain. In the applications to radar imaging, CS based radar is studied to reconstruct high resolution images with a small amount of measurements [8–10]. In this proposed CS-based MIMO array platform, we aim to resolve the issue of mutual inference in MIMO operation by reducing the number of transmit channels. In particular, instead of fixing the transmit antennas as conventional MIMO radars do, we randomly select the restricted number of transmit antennas for each signal transmission such that compressive measurements of the full channel MIMO operation can be made. This randomization of transmit channels ensures that the linear measurements fully capture the scene information. As regarding to the motion errors, we assume they are known or can be estimated accurately. Under this assumption, we treat them as a complementary source of randomness to favor CS reconstruction. A CS-based imaging approach is then employed to reconstruct the 3D reflectivity of interest using these random measurements.

Our platform with randomized transmit channels provides significant advantages over the conventional MIMO radar systems with fixed channels. First, the imaging performance of our system is comparable to that using full MIMO channel operation, but with much fewer transmit channels, which reduces channel interferences and saves time and expense for data collection. Second, with our CS-based imaging method, we are able to suppress the ambiguity caused by speed variations and motion errors with improved imaging resolution.

2. MODEL OF MOVING MIMO ARRAY

We consider a 3D configuration in the range-azimuth-elevation (x-y-z) space where a coherent MIMO radar is mounted on a moving platform to illuminate an area of interest. The MIMO radar is composed of a physical uniform linear array of N transmit-receive antennas along the elevation direction with half-wavelength spacing between adjacent antennas. As the MIMO radar platform moves in the azimuth direction, a virtual planar aperture is formed in the azimuth-elevation plane with 3D imaging capability. For simplicity, we assume the moving MIMO array operates in the spotlight mode, *i.e.*, it illuminates the same area of interest across its whole track. Let the source pulse transmitted by the antenna located at $\boldsymbol{r}_t = (x_t = 0, y_t, z_t)$ be p, and its frequency spectrum be P given by

$$P(\omega) = \int p(t) e^{-\mathrm{j}\omega t}\,\mathrm{d}t, \tag{1}$$

where $\omega = 2\pi f$ represents the angular frequency. The received echo at $\boldsymbol{r}_r = (x_r = 0, y_r = y_t, z_r)$ reflected by the area due to pulse p emitted at $\boldsymbol{r}_t$ can be approximated by

$$s(t, y_t, z_t, z_r) = \int \frac{1}{4\pi\|\boldsymbol{r}-\boldsymbol{r}_t\|_2^2} \cdot \frac{1}{4\pi\|\boldsymbol{r}-\boldsymbol{r}_r\|_2^2} f(\boldsymbol{r}) \\ p\left(t - \frac{\|\boldsymbol{r}-\boldsymbol{r}_t\|_2 + \|\boldsymbol{r}-\boldsymbol{r}_r\|_2}{c}\right)\mathrm{d}\boldsymbol{r}, \tag{2}$$

where $f(\boldsymbol{r})$ is the reflectivity at $\boldsymbol{r} = (x, y, z)$, $\|\cdot\|_2$ denotes the Euclidean distance, and c is the speed of light in the free space. After range compression, the received echo can be presented in the frequency domain by

$$S(\omega, y_t, z_t, z_r) = P^*(\omega) \int s(t, y_t, z_t, z_r) e^{-\mathrm{j}\omega t}\,\mathrm{d}t. \tag{3}$$

The 3D spatial Fourier transform of the range-compressed echo can be expressed in the ω–k space as

$$S(\omega, k'_y, k'_{zt}, k'_{zr}) = P^*(\omega) \int_{\mathbb{R}^4} s(t, y_t, z_t, z_r) \\ e^{-\mathrm{j}(\omega t + k'_y y_t + k'_{zt} z_t + k'_{zr} z_r)}\,\mathrm{d}t\,\mathrm{d}y_t\,\mathrm{d}z_t\,\mathrm{d}z_r. \tag{4}$$

Using the method of stationary phase [11] and by redefining the temporal origin to be centered at the 3D image cubic center $\boldsymbol{r}_0 = (x_0, y_0, z_0)$, the equation (4) evaluates to

$$\begin{aligned} & S(\omega, k'_y, k'_{zt}, k'_{zr}) \\ \propto\ & P^*(\omega)P(\omega)e^{-\mathrm{j}\langle \boldsymbol{k}, \boldsymbol{r}_0\rangle + 2k\|\boldsymbol{r}_0\|_2} \int_{\mathbb{R}^3} f(\boldsymbol{r}) e^{-\mathrm{j}\langle \boldsymbol{k}, \boldsymbol{r}\rangle}\,\mathrm{d}\boldsymbol{r} \\ =\ & P^*(\omega)P(\omega)e^{-\mathrm{j}\langle \boldsymbol{k}, \boldsymbol{r}_0\rangle + 2k\|\boldsymbol{r}_0\|_2} \mathcal{F}\{f(\boldsymbol{r})\}(\boldsymbol{k}), \end{aligned} \tag{5}$$

where $\mathcal{F}$ denotes the 3D Fourier transform, and

$$\begin{aligned} & \boldsymbol{k} = (k_x, k_y, k_z),\ \langle \boldsymbol{k}, \boldsymbol{r}_0\rangle = k_x x_0 + k_y y_0 + k_z z_0, \\ & k_x = \sqrt{(\sqrt{k^2 - (k'_{zt})^2} + \sqrt{k^2 - (k'_{zr})^2})^2 - (k'_y)^2}, \\ & k_y = k'_y,\ k_z = k'_{zs} + k'_{zr},\ k = \omega/c. \end{aligned} \tag{6}$$

The forward process, described in (5), models the data acquisition as a function of the area reflectivity in the ω–k space. Using (5), the radar echoes can be efficiently computed using the fast Fourier transform given uniform spaced antennas and a uniform gridded reflectivity map.

When there exist motion errors, we replace the transmit-receive locations $\boldsymbol{r}_{t,r}$ in (2) with

$$\boldsymbol{r}'_{t,r} = \boldsymbol{r}_{t,r} + \Delta\boldsymbol{r}, \tag{7}$$

and make changes accordingly on (3)-(5). To efficiently simulate the data using the fast Fourier transform, we refine the spatial grid such that all elements of the virtual planar array lie in the grid points even with motion errors.

In the inverse process, we treat the moving MIMO data in its entirety to generate a 3D reflectivity map. We note that equation (5) also indicates that the reflectivity map f can be expressed as the inverse Fourier transform of the collected raw data. The corresponding adjoint process for image reconstruction of the 3D reflectivity can be approximated by

$$f(\boldsymbol{r}) \propto \mathcal{F}^{-1}\left\{S(\omega, k'_y, k'_{zt}, k'_{zr})P^*(\omega)P(\omega)e^{\mathrm{j}\langle \boldsymbol{k}, \boldsymbol{r}_0\rangle - 2k\|\boldsymbol{r}_0\|_2}\right\}. \tag{8}$$

Thus, the image of the reflectivity can be efficiently recovered using the 3D inverse Fourier transform in the ω–k space. Note that to use (8) for reconstruction, the data acquired over $(\omega, k'_y, k'_{zt}, k'_{zr})$ first needs to be weighted and rearranged into a 3D format over $\boldsymbol{k}$. This is done via the dispersion relation defined in (6) using a 3D Stolt mapping.

3. CS-BASED 3D IMAGING

To better describe our CS-based 3D imaging algorithm, we compactly denote the forward process in (5) as a linear transformation

$$\mathbf{s} = \mathbf{\Phi}\mathbf{f}, \tag{9}$$

where $\mathbf{s}$, $\mathbf{\Phi}$, and $\mathbf{f}$ represent the received signal, the forward acquisition process, and the 3D ground reflectivity in the matrix-vector form, respectively. The corresponding adjoint process for inverse imaging is described by

$$\mathbf{f} = \mathbf{\Phi}^H\mathbf{s}. \tag{10}$$

With randomized transmit channels and known discretized motion errors, the echoes acquired by the proposed system can be simulated by subsampling the raw data collected by antennas on refined uniform grid points, according to the transmit-receive antenna locations. We denote the subsampling operator with $\mathbf{M}$. Thus, the acquired echoes can be represented as a linear transform of $\mathbf{f}$

$$\mathbf{u} = \mathbf{M}\mathbf{s} = \mathbf{M}\mathbf{\Phi}\mathbf{f} = \mathbf{\Psi}\mathbf{f}. \tag{11}$$

Considering the sparse property of radar images, we decompose $\mathbf{f}$ into a sparse component $\mathbf{f}_s$ and a dense residual $\mathbf{f}_r$. The sparse component $\mathbf{f}_s$ is estimated by solving the following minimization problem that promotes image-domain sparsity

$$\widehat{\mathbf{f}}_s = \arg\min_{\mathbf{f}} \|\mathbf{u} - \mathbf{\Psi}\mathbf{f}\|_2^2 \text{ s.t. } \|\mathbf{f}\|_0 < T. \tag{12}$$

The residual due to the dense component can be computed using the sparse estimate, *i.e.*, $\mathbf{u}_r = \mathbf{u} - \mathbf{\Psi}\widehat{\mathbf{f}}_s$. Theoretically the dense component can be estimated using least squares with the pseudo-inverse of $\mathbf{\Psi}$ as $\mathbf{\Psi}^\dagger\mathbf{u}_r$. However, due to the size of $\mathbf{\Psi}$, the pseudo-inverse $\mathbf{\Psi}^\dagger$ is impossible to compute directly. Therefore, we rely on the adjoint with a line search to estimate the dense part as follows

$$\widehat{\mathbf{f}}_r = \frac{\mathbf{u}_r^H\mathbf{u}_r}{\mathbf{u}_r^H\mathbf{\Psi}\mathbf{\Psi}^H\mathbf{u}_r}\mathbf{\Psi}^H\mathbf{u}_r. \tag{13}$$

Inspired by STOMP [12], we use an iterative algorithm to efficiently estimate the sparse part $\widehat{\mathbf{f}}_s$. First a residual vector is initialized from the measurements, $\mathbf{u}_r^{(0)} = \mathbf{u}$, with $\widehat{\mathbf{f}}_s^{(0)} = \mathbf{0}$. Each iteration, i, uses the residual $\mathbf{u}_r^{(i-1)}$ to estimate the signal $\tilde{\mathbf{f}}^{(i)}$ that was not explained yet. A threshold $\tau^{(i)}$, which is a fraction of the largest in magnitude component, is then applied to hard threshold $\tilde{\mathbf{f}}^{(i)}$ by setting all components less than $\tau^{(i)}$ in magnitude to zero. The remaining strongest reflectors $\mathbf{d}^{(i)}$ are scaled to capture most of the residual energy in $\mathbf{u}_r^{(i-1)}$, and added to the overall signal estimate from the previous iteration $\widehat{\mathbf{f}}_s^{(i-1)}$ to produce the current signal estimate $\widehat{\mathbf{f}}_s^{(i)}$. The residual $\mathbf{u}_r^{(i-1)}$ is updated and the algorithm iterates until the relative reconstruction error is smaller than a preset small value ϵ. The final image $\widehat{\mathbf{f}}$ combines the sparse part of previous iterations and the dense part estimate. More details about this algorithm are available at [13].

4. SIMULATIONS

To verify our approach, we consider a cross-track moving MIMO array in the azimuth-elevation plane illuminating a synthetic half cylinder-shaped object. For comparison, we consider three MIMO platforms in simulation: (1) a benchmark full-channel platform moving along a straight-line track with a constant speed as shown in Fig.1(a), (2) a conventional moving platform with a restricted number of fixed transmit channels as shown in Fig.1(b), and (3) our proposed platform with randomized transmit channels as presented in Fig.1(c).

In particular, for the benchmark MIMO array platform, we consider an ideal uniform linear array of 12 transmit-receive antennas with full channel operation along its moving track. For the second platform, we use the two end antennas as the transmit channels to reduce mutual interference and all the 12 antennas as receive antennas. For fair comparison, we consider the same aperture size as the benchmark platform, but with non-uniform virtual array due to motion errors. The motion errors are discretized using unit of half element spacing, and only translational motion errors are considered to simplified our simulation. For our proposed MIMO array platform, we consider the same aperture size, the same motion errors and the same number of transmit channels as the second platform, except with randomized transmit antennas.

To unify the simulations of the aforementioned three platforms, we simulate data using a refined virtual MIMO array in the azimuth-elevation plane in which all elements of the three platforms can be found correspondingly. For the benchmark 12-channel MIMO operation, we uniformly downsample the noiseless simulated data in azimuth and elevation directions according to the ideal locations of transmit-receive antennas. For the conventional MIMO array platform and our proposed MIMO array platform, we add white Gaussian noise to the simulated time-domain data with a peak signal-to-noise ratio of 30dB, and then downsample the noisy data corresponding to the 2 transmit antennas, either fixed or randomly picked, and all 12 receive antennas with motion errors.

Assuming all the data are perfectly aligned, we consider two imaging methods: the conventional ω–k imaging method described in Section 2, and the CS-based imaging approach presented in Section 3. The imaging results of the synthetic object are shown in Fig. 2. From left to right, we plot the imaging results using (a) the conventional imaging method on ideal linear motion track and noise-free data of full MIMO operation, (b) the conventional imaging method on noisy data of 2 fixed transmit channels with motion errors, and (c)the CS-based iterative reconstruction method on noisy data of 2 random transmit channels with the same motion errors of (b). As evident in the Fig. 2, the imaging result using idealized data collection clearly retrieves the 3D object in the 3D space. However, for the conventional system with a restricted number of transmit channels and motion errors, the imaging result is significantly degraded and exhibits ambiguity in both the azimuth and elevation directions. While with our random transmit channel scheme incorporated with the CS imaging approach, the imaging result is significantly improved, with about 11dB SNR improvement if we treat the benchmark imaging result as the noise-free signal in SNR computation. Our result is also very close to that using ideal full channel MIMO operation but with much fewer transmit channels, which reduces potential mutual interference of channels and cost of data collection.

5. CONCLUSION

We propose a compressive sensing based moving MIMO radar platform using randomized transmit channels to overcome the challenges of transmit channel reduction due to mutual interference and compensation of motion errors. Imaging results with simulated data demonstrate that we are able to reconstruct a high resolution 3D image similar to that of the

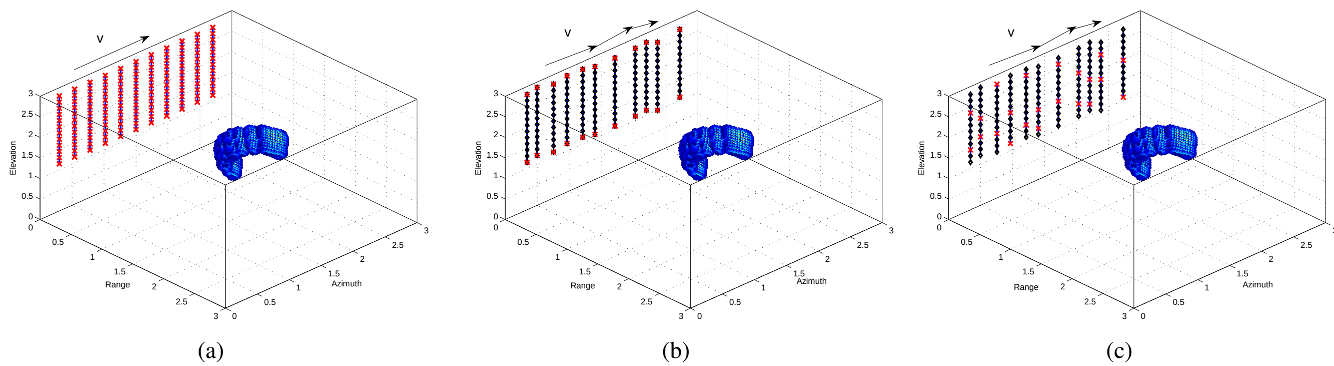

Fig. 1. Moving MIMO array of (a) ideal full-channel, (b)2 fixed transmit channels with motion errors, and (c)2 randomized transmit channels with motion errors. Red x represent transmit-receive channels and black dots represent receive channels.

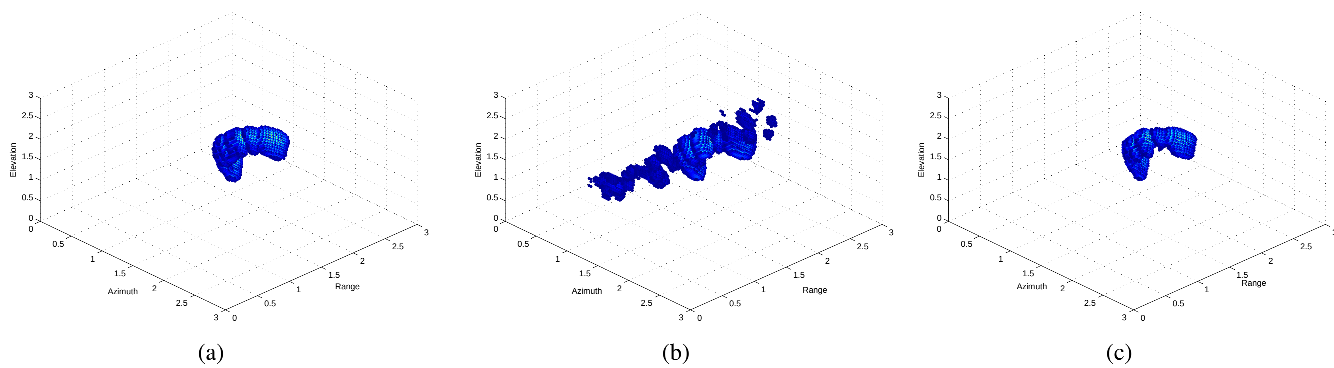

Fig. 2. Imaging results using (a) noise-free data collected by ideal full-channel moving MIMO, (b) noisy data collected by practical moving MIMO with 2 fixed transmitters, and(c) CS based moving MIMO with 2 randomized transmitters.

ideal full-channel MIMO array, but with much fewer transmit channels. Compared to the conventional moving MIMO array with fixed transmit channels, our CS-based platform performs significantly better with reduced ambiguity.

6. REFERENCES

[1] G. Fornaro, F. Serafino, and F. Soldovieri, "Three-dimensional focusing with multipass SAR data," *IEEE Trans. Geoscience and Remote Sensing*, vol. 41(3), pp. 507–517, March 2003.

[2] Z. Yang, M. Xing, G. Sun, and Z. Bao, "Joint multichannel motion compensation method for MIMO SAR 3D imaging," *International Journal of Antenna and Propagation*, 2014.

[3] W. Wang, "Virtual antenna array analysis for MIMO synthetic aperture radars," *International Journal of Antenna and Propagation*, 2012.

[4] X. Zhuge and A. G. Yarovoy, "A sparse aperture MIMO-SAR-based UWB imaging system for concealed weapon detection," *IEEE Trans. Geoscience and Remote Sensing*, vol. 49(1), pp. 509–518, January 2011.

[5] G. Krieger, "MIMO-SAR: opportunities and pitfalls," *IEEE Trans. Geoscience and Remote Sensing*, vol. 52(5), pp. 2628–2645, May 2014.

[6] G. Krieger, M. Younis, S. Huber, F. Bordoni, A. Patyuchenko, J. Kim, P. Laskowski, M. Villano, T. Rommel, P. Lopez-Dekker, and A. Moreira, "MIMO-SAR and the orthogonality confusion," in *IEEE International Geoscience and Remote Sensing Symposium (IGARSS)*, 2012, pp. 1533–1536.

[7] E. Candes, J. Romberg, and T. Tao, "Robust uncertainty principles: Exact signal reconstructoin from highly incomplete frequency information," *IEEE Transactions on Information Theory*, vol. 52(2), Februray 2006.

[8] R. Baraniuk and P. Steeghs, "Compressive radar imaging," in *IEEE Radar Conference*, MA, April 2007.

[9] M. A. Herman and T. Strohmer, "High-resolution radar via compressed sensing," *IEEE Trans. Signal Process.*, vol. 57, June 2009.

[10] L. C. Potter, E. Ertin, J. T. Parker, and M. Cetin, "Sparsity and compressed sensing in radar imaging," *Processings of the IEEE*, vol. 98, pp. 1006–1020, June 2010.

[11] M. Born and E. Wolf, *Principles of optics*, Cambridge University press, 1999.

[12] D.L. Donoho, Y. Tsaig, I. Drori, and J.-L. Starck, "Sparse solution of underdetermined systems of linear equations by stagewide orthogonal matching pursuit," *IEEE Trans. Information Theory*, Februray 2012.

[13] D. Liu and P. T. Boufounos, "Compressive sensing based 3d sar imaging with multi-prf baselines," in *IEEE International Geoscience and Remote Sensing Symposium(IGARSS)*, 2014.